Clays and Clay Minerals, Vol. 53, No. 6, 557–563, 2005.

EFFECTS OF SIDEROPHORES ON Pb AND Cd ADSORPTION TO KAOLINITE

SARAH E. HEPINSTALL, BENJAMIN F. TURNER AND PATRICIA A. MAURICE*
Department of Civil Engineering & Geological Sciences, University of Notre Dame, Notre Dame, IN 46556, USA

Abstract—Siderophores are low molecular weight organic ligands synthesized by aerobic microorganisms to acquire Fe. In addition to Fe(III), siderophores may complex other metals such as Pb and Cd. This study compared the effects of the trihydroxamate siderophores desferrioxamine-B (DFO-B), desferrioxamine-D_1 (DFO-D_1), desferrioxamine-E (DFO-E), and the monohydroxamate siderophore-like ligand acetohydroxamic acid (aHA) on Pb and Cd (except for DFO-E) adsorption to kaolinite (KGa-1b) at pH 4.5 to 9, in 0.1 M $NaClO_4$, at 22ºC, in the dark. At pH >6, all of the studied ligands decreased Pb adsorption to kaolinite: aHA by 5–40% and DFO-B, DFO-D_1 and DFO-E by 30–75%; the greater effects were at higher pH. The studied ligands decreased Cd adsorption to kaolinite at pH >8: aHA by 5–20% and the trihydroxamates by as much as 80%. We also observed enhancement of Pb adsorption in the presence of DFO-B at pH ~5–6.0, probably due to adsorption of the doubly positively charged $H_3Pb(DFO\text{-}B)^{2+}$ complex, although spectroscopic evidence is needed.

Key Words—Adsorption, Cadmium, Kaolinite, Lead, Ligand, Siderophore.

INTRODUCTION

Siderophores are low molecular weight organic ligands produced by microorganisms and some plants under Fe-limited conditions, and commonly present in soil systems (Neilands, 1981; Kraemer, 2004). Siderophores have a high specificity for Fe(III), relative to Fe(II); siderophore Fe(III) 1:1 complex stability constants range from 10^{23} to 10^{52} (Neilands, 1981; Crumbliss, 1991). Siderophores can also form stable complexes with other metals, such as Al(III), Ga(III), In(III), Cd(II) and Pb(II) (Anderegg *et al*., 1963; Evers *et al*., 1989; Hernlem *et al*., 1996). This ability to form stable metal-ligand complexes suggests that siderophores may influence metal mobility in soils by affecting rates of mineral weathering (Hersman *et al*., 1995; Holmén and Casey, 1996; Liermann *et al*., 2000; Kalinowski *et al*., 2000; Cervini-Silva and Sposito, 2002; Rosenberg and Maurice, 2003), and/or by either enhancing or inhibiting metal adsorption (Kraemer *et al*., 1999, 2002; Neubauer *et al*., 2000). Potential co-adsorption of siderophore-metal complexes to the mineral-surface might enhance metal adsorption. Alternatively, if siderophores in solution compete with mineral surface adsorption sites, or if metal-siderophore complexes adsorb less strongly than the metals alone, then metal adsorption may be inhibited.

One of the main groups of siderophores is the hydroxamates. Hydroxamate functional groups on siderophores can form solution complexes with Fe(III) upon loss of a proton from the hydroxylamine group and bidentate bonding with the carbonyl and hydroxylamine groups. This complexation results in a five-membered ring (Crumbliss, 1991; Kraemer, 2004). Hydroxamate siderophores generally contain three hydroxamate functional groups (*i.e.* trihydroxamate). The six O ligands in this arrangement satisfy the favored octahedral coordination of Fe(III) (Hersman *et al*., 1995). This makes the siderophores highly Fe(III) specific, rather than Fe(II), and stable in the complex (Hersman *et al*., 1995). Trihydroxamate siderophores have properties that need to be considered that are not present in monohydroxamate acids, such as the length of space on the molecule between the hydroxamate functional groups, the rigidity and orientation of the atoms between the functional groups, and the relative orientation of the functional groups (Crumbliss, 1991). The stability constants of Fe-hydroxamate siderophore complexes appear to depend, at least in part, on the number of hydroxamate groups bound to Fe^{3+} (Crumbliss, 1991).

This research compared: (1) the effects of a monohydroxamate siderophore-like ligand (acetohydroxamic acid, aHA) and three trihydroxamate siderophores (desferrioxamine-B, DFO-B; desferrioxamine-D_1, DFO-D_1; and desferrioxamine-E, DFO-E) on Pb adsorption to kaolinite as a function of pH and metal concentration; and (2) the effects of aHA, DFO-B and DFO-D_1 on Cd adsorption to kaolinite as a function of pH and metal concentration. Batch adsorption experiments were conducted to characterize Pb and Cd adsorption to kaolinite alone and in ternary systems (*i.e.* metal-siderophore-kaolinite).

The siderophore-like ligand aHA (Figure 1a) is monohydroxamate, meaning that it has only one hydroxamate functional group on its molecule to bind Fe(III). The aHA ligand is uncharged at pH < 9 (Holmén *et al*., 1997), and has a stability constant with Fe(III) of $10^{11.48}$ (Anderegg *et al*., 1963). DFO-B, DFO-D_1 and DFO-E each have three functional groups on their molecules

* E-mail address of corresponding author:
pmaurice@nd.edu
DOI: 10.1346/CCMN.2005.0530601

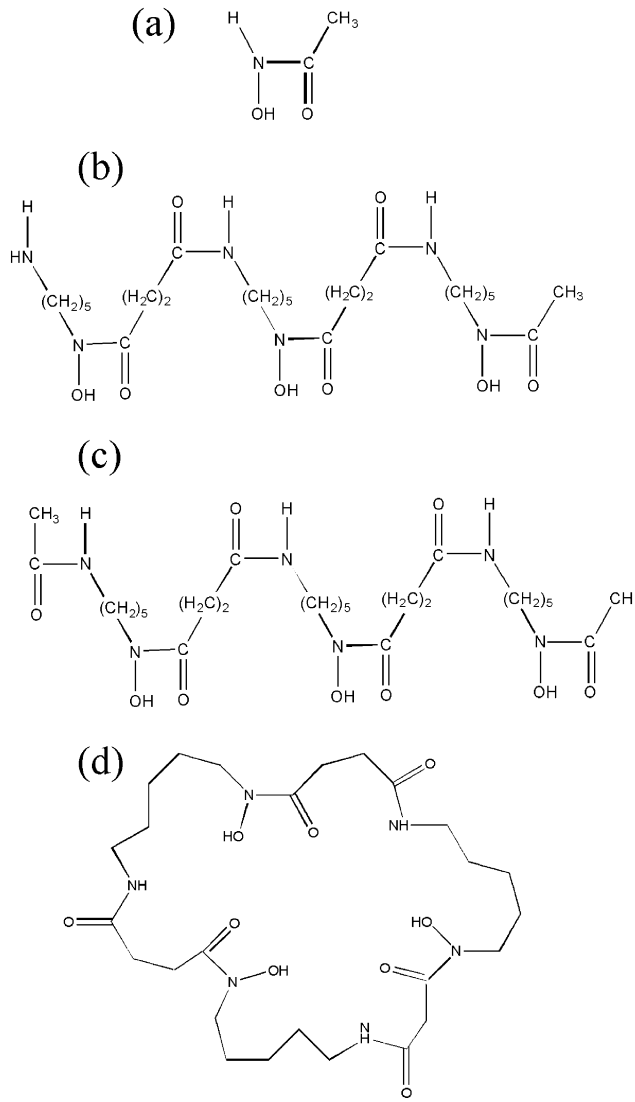

Figure 1. Molecular structure of (a) aHA (siderophore-like monohydroxamate), (b) DFO-B (linear trihydroxamate), (c) DFO-D_1 (linear trihydroxamate), and (d) DFO-E (cyclic trihydroxamate).

with which to bind Fe(III), and have higher stability constants with Fe(III) than does aHA. DFO-B (Figure 1b) is a positively charged biomolecule at pH <8 (Borgias *et al.*, 1989). In DFO-D_1 (Figure 1c), an acetyl group replaces the proton on the terminal amine group of the DFO-B molecule, thus making DFO-D_1 uncharged at most pH values (Kraemer *et al.*, 1999). DFO-E is compositionally similar to DFO-B, but it is cyclic rather than linear (Figure 1d); it is uncharged (neutral) (Ruggiero *et al.*, 2002).

MATERIALS AND METHODS

Kaolinite

The kaolinite sample used in this research was The Clay Minerals Society Source Clay KGa-1b. The kaolinite was cleaned prior to batch adsorption experiments, according to the procedure described by Sutheimer *et al.* (1999). The clay was then washed with Milli-Q® UV (ultraviolet)-treated deionized water until the conductivity of the supernatant liquid was <300 µS/cm, and freeze dried for storage prior to experimentation.

The BET surface area measured on a SA 3100 volumetric sorption analyzer from Coulter Instruments, Inc., using N_2 adsorption in the method, was 12.1 m^2/g. The point of zero net proton charge (pH_{pznpc}) for KGa-1b is 5.1 ± 0.2 (Sutheimer *et al.*, 1999).

Siderophores

The aHA was obtained from Sigma Aldrich. DFO-B also was obtained commercially through Sigma Aldrich,

https://doi.org/10.1346/CCMN.2005.0530601 Published online by Cambridge University Press

in mesylate salt form. DFO-D_1 was synthesized from DFO-B by per-acetylation in methanol. Hydrolysis of the hydroxamate esters of the per-acetylated DFO-B with ammonia was completed according to the procedure described by Kraemer *et al.* (1999) in the University of Notre Dame laboratory of Dr Marvin Miller of the Department of Chemistry and Biochemistry. The resulting solid was tested for composition and purity on a Varion Unity Plus 300 MHz nuclear magnetic resonance (NMR) spectrometer located in the Department of Chemistry at the University of Notre Dame. DFO-E was obtained courtesy of Dr Larry Hersman; the DFO-E had been isolated from a *Streptomyces olivaceus* strain in the laboratory of G. Winkelmann at the Department of Microbiology and Biotechnology, University of Tübingen, Germany, in the manner described by Meiwes *et al.* (1990) and Konetschny-Rapp *et al.* (1992).

Batch adsorption experiments

Both adsorption envelopes (adsorption as a function of pH) and adsorption isotherms (at one pH, as a function of metal concentration) were completed in 0.1 M $NaClO_4$ background electrolyte. Clean KGa-1b (0.0516 g) powder was weighed and added to 28 mL of acid-washed Nalgene polypropylene centrifuge tubes; each sample had an eventual solid (KGa-1b) concentration of 2.064 g L^{-1}. The metal stock solutions were made with $Pb(NO_3)_2$ or $Cd(NO_3)_2$ ICP-OES standard and mixed with the electrolyte (0.1 M $NaClO_4$) to obtain a metal concentration of 11.1 μM. The powdered siderophore was also added to this solution to attain 240 μM. The total solution volume of each centrifuge tube was 25 mL. The pH of each sample was adjusted with 0.01 M to 0.1 M NaOH and 0.01 M HCl; the pH range for the adsorption envelopes was 4.5 to 8 for samples containing Pb without added siderophores and 4.5 to 9 for all other samples. The Pb envelope in the absence of siderophores was only run to pH 8 in order to avoid potential saturation with respect to $PbCO_3$ and $Pb(OH)_2$ phases, as predicted by modeling with PHREEQC. Although saturation with respect to $Pb(OH)_2$(s) was approached at pH 8, there was no evidence for precipitation at this pH, even upon comparing 0.1 μm filtered and unfiltered solutions.

The samples were run in triplicate, along with a control containing no kaolinite. The samples were shaken using a Labquake rotisserie shaker for 2 h in the dark at 22ºC. After 2 h, the pH was recorded; pH changes were within ±0.3 units. Previous studies showed that this was ample time to achieve adsorption equilibrium (Neubauer *et al.*, 2000). The samples were centrifuged using a Fisher Scientific Marathon 21000 Centrifuge at 9000 rpm for 5 min, filtered with a 0.2 μm Millipore PTFE filters, stored in polystyrene centrifuge tubes and glass vials, and refrigerated until analysis. Adsorption edges were completed for Pb in the presence and absence of the siderophores aHA, DFO-B, DFO-D_1 and DFO-E. Adsorption edges for Cd were completed in the presence and absence of aHA, DFO-B and DFO-D_1; we did not have enough DFO-E for use with Cd. Calculations of adsorption edges and isotherms were based on the control sample concentration minus the concentration remaining in solution after the solid was separated from the solution in reacted samples.

Batch adsorption isotherm experiments were conducted in 0.1 M $NaClO_4$ background electrolyte; the metal concentrations ranged from 10^{-7} to $10^{-4.15}$ M for Pb isotherms at pH 5 and 6 and 10^{-7} to $10^{-4.5}$ M for the Pb isotherms at pH 8 and Cd isotherms. KGa-1b had a solid concentration of 2.064 g L^{-1}; the siderophore concentration was either 0 or 240 μM. Samples were run in triplicate, as well as non-kaolinite-containing controls at each metal concentration. Pb isotherms were performed at pH 5, 6 and 8 with aHA, DFO-B and DFO-D_1. Cd isotherms, at pH 5, 8 and 9, were also completed with aHA, DFO-B and DFO-D_1.

Metal and organic carbon analysis

Perkin Elmer inductively coupled plasma optical emission spectrometers (ICP-OES) Optima 3300 XL and Optima 2000 DV were used to measure the aqueous metal concentrations remaining in solution after adsorption reactions and in non-kaolinite-containing controls. Fe, Si and Al concentrations also were analyzed on the ICP-OES for the adsorption-edge experiments to determine whether there was an increase in the dissolution of KGa-1b in the presence of the siderophores. Within error, there was little to no increase in Fe or Al aqueous concentrations in the siderophore-containing samples compared to the non-siderophore controls. Fe release was <5 ppb; Al release ranged from 5 to 15 ppb. The Si concentrations were below the detection limit of the ICP-OES (10 ppb).

Dissolved organic carbon (DOC) concentrations were measured on a Shimadzu TOC-5000 analyzer. The amount of siderophore adsorbed was calculated by difference between control and kaolinite-reacted samples.

The DFO-B used in the experiments was in mesylate salt form; the mesylate ions contained carbon that was measured along with the DFO-B carbon concentrations. However, the mesylate/DFO-B carbon ratio per molecule is 1:25, so that the effect on measured DFOB concentrations was small ($\leqslant$4%) (Rosenberg and Maurice, 2003).

The modeling program PHREEQC version 2 (Parkhurst and Appelo, 1999) was used to model metal speciation in solution, with constants provided in Table 1. The CO_2 partial pressure of $10^{-3.5}$ was assumed in all speciation calculations. The Pb carbonate and Cd carbonate complexes were not plotted in the results because they were present at very small concentrations. The highest concentration of Pb carbonate determined by the simulation was at pH 10 and was only 2.0% of the total Pb; the Cd carbonate concentrations were much lower percentages.

https://doi.org/10.1346/CCMN.2005.0530601 Published online by Cambridge University Press

Table 1. Siderophore-metal log stability constants used in modeling.

Reaction	Log stability constant[a]
DFO-B and aHA	
$(DFOB)^{3-} + H^+ = H(DFOB)^{2-}$	10.90[b]
$(DFOB)^{3-} + 2H^+ = H_2(DFOB)^-$	20.48[b]
$(DFOB)^{3-} + 3H^+ = H_3(DFOB)$	29.48[b]
$(DFOB)^{3-} + 4H^+ = H_4(DFOB)^+$	37.85[b]
$Pb^{2+} + (DFOB)^{3-} + H^+ = HPb(DFOB)$	20.87[b]
$Pb^{2+} + (DFOB)^{3-} + 2H^+ = H_2Pb(DFOB)^+$	29.73[b]
$Pb^{2+} + (DFOB)^{3-} + 3H^+ = H_3Pb(DFOB)^{2+}$	35.40[b]
$2\ Pb^{2+} + H(DFOB)^{2-} = HPb_2(DFOB)^{2+}$	16.29[b]
$Cd^{2+} + (DFOB)^{3-} + H^+ = HCd(DFOB)$	18.8[c]
$Cd^{2+} + (DFOB)^{3-} + 2H^+ = H_2Cd(DFOB)^+$	26.0[c]
$Cd^{2+} + (DFOB)^{3-} + 3H^+ = H_3Cd(DFOB)^{2+}$	32.7[c]
$(aHA)^- + H^+ = H(aHA)^0$	9.29[d]
$Cd^{2+} + (aHA)^- = Cd(aHA)^+$	4.5[d]
$Cd^{2+} + 2(aHA)^- = Cd(aHA)_2^0$	7.8[e]
$Pb^{2+} + (aHA)^- = Pb(aHA)^+$	6.7[d]
$Pb^{2+} + 2(aHA)^- = Pb(aHA)_2^0$	10.7[e]

[a] All stability constants determined at a background electrolyte concentration of 0.1 M
[b] Hernlem *et al.* (1996)
[c] Neubauer *et al.* (2000)
[d] Martell and Smith (2001)
[e] Anderegg *et al.* (1963)

RESULTS AND DISCUSSION

Adsorption envelopes

In the absence of siderophores, 5–25% of Pb (11.1 μM) adsorbed to kaolinite between pH 4.5 and 6 (Figure 2a). However, at pH >6, adsorption increased steadily until pH 8, at which point 80% of the initial aqueous Pb was adsorbed to the kaolinite surface.

The presence of aHA decreased Pb adsorption to kaolinite at pH ⩾6 by 5–40% (Figure 2b). The trihydroxamate siderophores decreased adsorption by 30–75% at pH 6.5–8. At pH ~4.5–6, it appeared that DFO-B and DFO-D_1 slightly but significantly enhanced Pb adsorption. As described below, Pb adsorption isotherms at pH 5 and 6 were completed in order to investigate more thoroughly the effects of siderophores on Pb adsorption in this pH range.

In the absence of siderophores, Cd (11.1 μM) adsorbed very little to kaolinite at pH <7 (Figure 2a). However, at pH >8, Cd adsorption increased. At pH 9, almost all of the Cd adsorbed to the kaolinite surface. The Cd adsorption edge was shifted to higher pH in comparison to the Pb adsorption edge.

In the presence of aHA, Cd adsorption at pH >8 decreased by 5–20% (Figure 2c). DFO-B and DFO-D_1 also decreased Cd adsorption (pH >8), but to a greater extent, to 80%. Neubauer *et al.* (2000) also showed that DFO-B decreased Cd adsorption to kaolinite at pH >7.5. At pH <8, siderophores had no effect on Cd adsorption to kaolinite. Cd (0–15%) adsorbed very little to the kaolinite surface in the pH range 4.5–8, regardless of the presence of siderophores.

Adsorption isotherms

The Pb adsorption isotherms at pH 5 (Figure 3a) confirmed that DFO-B and DFO-D_1 enhanced Pb adsorption, and showed that the most Pb adsorbed to kaolinite in the presence of DFO-B, followed by DFO-D_1. The presence of aHA had no effect on Pb adsorption. At pH 6, DFO-B enhanced adsorption (Figure 3b). DFO-D_1 and aHA had either little or no effect on Pb adsorption to kaolinite at this pH. At pH 8, Pb adsorption to kaolinite was the strongest in the absence of siderophores (isotherm not shown here). Equilibrium modeling with PHREEQC suggested that at the Pb total aqueous concentrations >20 μM used in this experiment, a $Pb(OH)_2$ phase was approaching, or approximately at, saturation. However, there were no observations of loss of Pb from solution controls, even upon filtration. The siderophore-containing solutions were all below saturation. DFO-B and DFO-D_1 inhibited Pb adsorption to a greater extent than did aHA at pH 8. These results were in agreement with the Pb adsorption envelope results.

The Cd-adsorption isotherms completed at pH 5, 8 and 9 agreed well with the adsorption envelope results and therefore are not shown here.

Siderophore adsorption

Under the experimental conditions, very little siderophore (aHA, DFO-B, or DFO-D_1) adsorbed to KGa-1b (data not shown here). The aHA adsorbed <1% to the kaolinite surface at pH 4.5–9. DFO-B adsorption to kaolinite ranged from 2–4%, was in agreement with the

https://doi.org/10.1346/CCMN.2005.0530601 Published online by Cambridge University Press

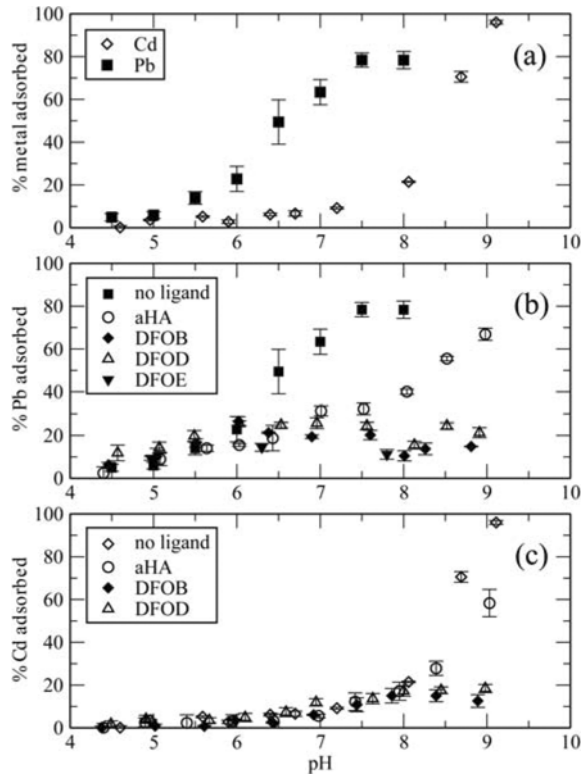

Figure 2. (a) Recent Pb and Cd sorbed as a function of pH. (b) Pb (11.1 μM) adsorption envelope to kaolinite in the presence and absence of siderophores (240 μM). (c) Cd (11.1 μM) adsorption in the presence and absence of siderophores (240 μM). Here and in Figure 3, aHA = acetohydroxamic acid, DFOB = DFO-B, DFOD = DFO-D_1 and DFOE = DFO-E (DFO is our abbreviation for desferrioxamine).

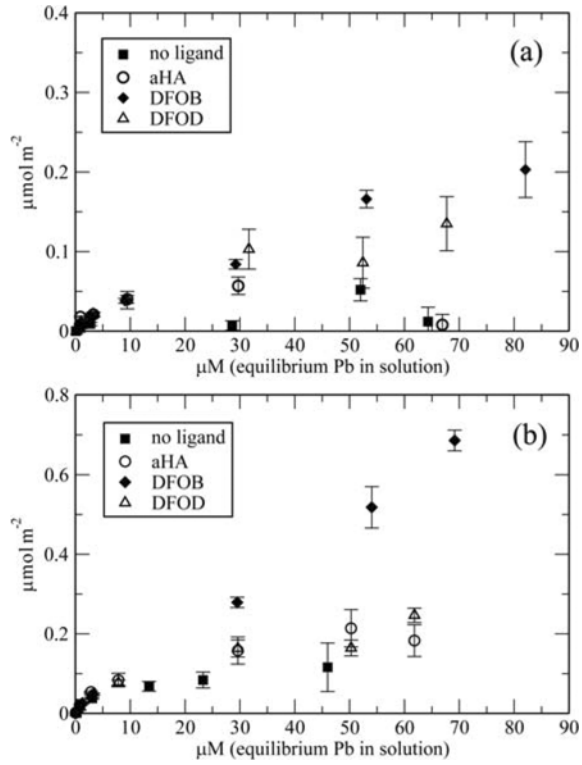

Figure 3. Pb adsorption isotherms. (a) Pb (10^{-7} to $10^{-4.15}$ M) adsorption isotherm at pH 5 in the absence and presence of siderophores (240 μM). (b) Pb (10^{-7} to $10^{-4.15}$ M) adsorption isotherm at pH 6 in the absence and presence of siderophores (240 μM).

observations of Neubauer *et al.* (2000), who found 1–5% adsorption of DFO-B to kaolinite (KGa-2). Because of the small to negligible percent adsorption, experimental error made it difficult to determine the exact amount adsorbed, or to discern any trend with pH. DFO-D_1 adsorbed slightly (2–7%) to kaolinite at pH 4.5 to 6.5; DFO-D_1 adsorbed slightly or not at all ($\leqslant$2%) at pH >7.

Evidence from solution speciation

In the absence of siderophores, Pb^{2+} is the dominant Pb species to pH 7; above pH 7, $Pb(OH)^+$ and $PbCO_3$ become increasingly important. Calculation of Pb solution speciation in the presence of aHA and DFO-B (Figure 4a,b) provides further insight into the potential mechanisms behind the effects of the various ligands on adsorption. Both aHA and DFO-B form complexes with Pb that become the dominant Pb species in solution at pH above ~6. Two aHA complexes, $aHAPb^+$ and aHA_2Pb, could potentially be responsible for the inhibition of Pb adsorption by this ligand (Figure 4a), either by competing with the kaolinite surface for Pb or by adsorbing to a lesser extent than the inorganic Pb species.

The high concentrations of two Pb/DFO-B complexes, H_2Pb $(DFO\text{-}B)^+$ and HPb(DFO-B), at pH 6–10 probably accounted for the greatly diminished Pb adsorption to KGa-1b observed at pH 6–8 (Figure 4b). Note that we did not perform adsorption experiments above pH 8 for Pb solutions without DFO-B because of solubility concerns.

A third complex, H_3Pb $(DFO\text{-}B)^{2+}$, occurred over a narrow pH range, beginning at ~pH 4.5 and essentially negligible by pH 7.5. The H_3Pb $(DFO\text{-}B)^{2+}$ complex may be an important factor in understanding the slight enhancement of Pb adsorption to KGa-1b at pH ~5–6, which is the pH range where this species is important. The pH_{pznpc} of kaolinite is 5.1. Thus, above this pH, the kaolinite surface has an overall net negative charge. The H_3Pb $(DFO\text{-}B)^{2+}$ complex was the most highly positively charged Pb species in solution in the pH range where enhanced adsorption was observed, and it might adsorb through electrostatic interactions, at least above pH 5.1. Adsorption to specific sites could also be important; however, deciphering the mechanisms of the observed enhanced adsorption, including any potential site-specificity, would require further spectroscopic studies.

Adsorption envelope data in Kraemer *et al.* (1999; their Figure 2) also suggested a slight enhancement of

https://doi.org/10.1346/CCMN.2005.0530601 Published online by Cambridge University Press

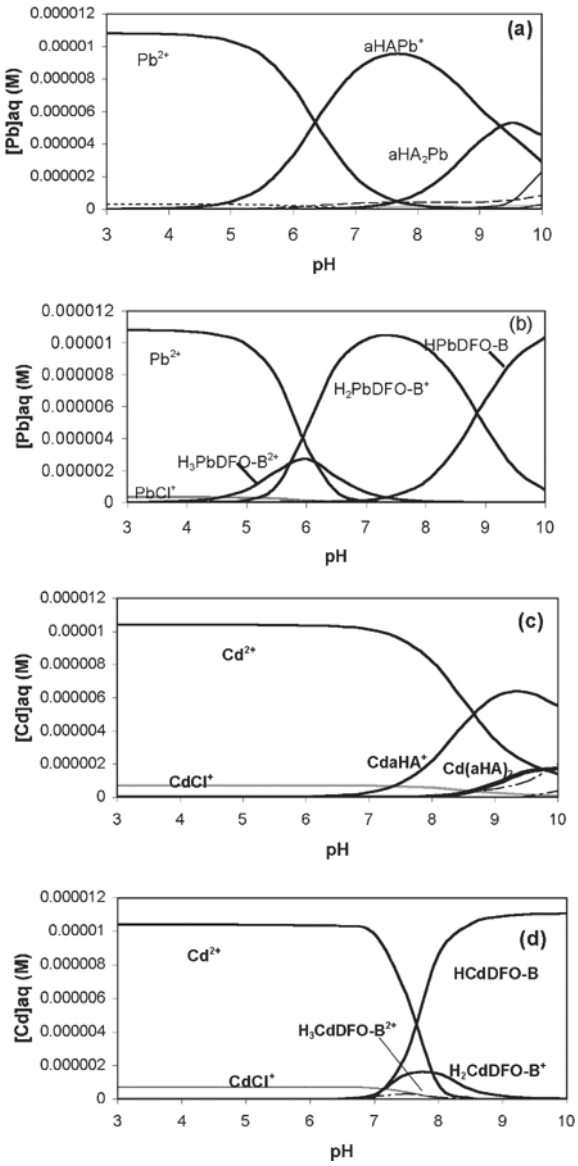

Figure 4. Metal (11.1 μM) species distribution diagrams. (a) Pb speciation in the presence of aHA. (b) Pb speciation in the presence of DFO-B. (c) Cd speciation in the presence of aHA. (d) Cd speciation in the presence of DFO-B.

Pb adsorption by DFO-B and DFO-D_1 to goethite at ~pH 5. However, this possibility was not explored, probably because the effect was small and limited to a narrow pH range.

Up to ~pH 8.5, Cd^{2+} was the dominant species; about this pH, $CdOH^+$ began to become important. The Cd/aHA system was similar to that of the Pb/aHA system except for the pH at which the metal/aHA complexes reached their peak concentrations (Figure 4c). Besides the difference in pH when parallel species dominated (Figure 4d), there was one primary difference between the Pb/DFO-B and Cd/DFO-B systems: the $H_3Pb(DFO\text{-}B)^{2+}$ complex had greater concentrations at pH 4.5–6 than the $CdH_3(DFO\text{-}B)^{2+}$ species did at any pH in the Cd/DFO-B system. This may explain, at least in part, why there was no enhancement in Cd adsorption by DFO-B at any pH studied here, although further study is needed.

CONCLUSIONS

This research demonstrated that siderophores may have an important impact on Pb and Cd mobility. The primary impact is decreased adsorption at intermediate to high pH. At pH >6, siderophores decreased Pb adsorption to kaolinite: aHA by 5–40% and DFO-B, DFO-D_1 and DFO-E decreased adsorption by 30–75%. Siderophores decreased Cd adsorption to kaolinite at pH >8: aHA by 5–20% and the trihydroxamates by as much as 80%. However, we also observed evidence that siderophores may, in some instances, enhance adsorption. We observed a slight increase in adsorption of Pb to kaolinite from pH ~5–6 in the presence of DFO-B and DFO-D_1. The slight enhancement in the presence of DFO-B was probably due to adsorption of the doubly positively charged $H_3Pb\ (DFO\text{-}B)^{2+}$complex, although spectroscopic evidence is needed to test this hypothesis.

The trihydroxamates affected metal adsorption similarly; aHA had a lesser effect on metal adsorption in comparison to the trihydroxamate siderophores, which all behaved in a broadly similar manner. The trihydroxamate siderophores tend to have greater metal-binding affinities than the monohydroxamic aHA. However, the molecular charge of the siderophore appears to have an additional effect on metal adsorption, given that DFO-B may have increased Pb adsorption at pH 4.5–6, perhaps through the $H_3Pb(DFO\text{-}B)^{2+}$complex. In any case, the effects of siderophores on metal adsorption to kaolinite appear to be sensitive to pH, metal identity, and the detailed structures and charge properties of the siderophores. This research suggests that siderophores have the ability to either enhance or inhibit metal mobility in porous media, and that further study encompassing a variety of siderophores, metals, mineral surfaces, solution conditions and including spectroscopic methods is needed.

ACKNOWLEDGMENTS

This research was funded by the National Science Foundation (Environmental Molecular Science Institute) and the Department of Energy (Basic Energy Science). The authors would also like to thank Dr Marvin Miller and Helen Zhu (Department of Chemistry and Biochemistry, University of Notre Dame) for assistance synthesizing DFO-D_1; Dr Larry Hersman (Los Alamos National Laboratory) for helpful discussion; G. Winkelman (Department of Microbiology and Biotechnology, University of Tübingen, Germany) for the DFO-E. We thank Dr Stephan Kraemer and an anonymous reviewer for detailed reviews that greatly improved the quality of the manuscript.

REFERENCES

Anderegg, G., L'Eplattenier, F. and Schwarzenbach, G. (1963) Hydroxamatkomplexe II. Die Anwendung der pH-methode. *Helvetica Chimica Acta*, **46**, 1400–1408.

Borgias, B., Hugi, A.D. and Raymond, K.N. (1989) Isomerization and solution structures of desferrioxamine B complexes of Al^{3+} and Ga^{3+}. *Inorganic Chemistry*, **28**, 3538–3545.

Cervini-Silva, J. and Sposito, G. (2002) Steady-state dissolution kinetics of aluminum-goethite in the presence of desferrioxamine-B and oxalate ligands. *Environmental Science and Technology*, **36**, 337–342.

Crumbliss, A. (1991) Aqueous solution equilibrium and kinetic studies of iron siderophore and model siderophore complexes. Pp. 177–233 in: *Handbook of Microbial Iron Chelates* (G. Winkelmann, editor). CRC Press, Boca Raton, Florida.

Evers, A., Hancock, R.D., Martell, A.E. and Motekaitis, R.J. (1989) Metal ion recognition in ligands with negatively charged oxygen donor groups. Complexation of Fe(III), Ga(III), In(III), Al(III) and other highly charged metal ions. *Inorganic Chemistry*, **29**, 2189–2195.

Fortin, D., Davis, B. and Beveridge, T.J. (1996) Role of Thiobacillus and sulfate-reducing bacteria in iron biocycling in oxic and acidic mine tailings. *FEMS Microbiology Ecology*, **21**, 11–24.

Hernlem, B.J., Vane, L.M. and Sayles, G.D. (1996) Stability constants for complexes of the siderophores desferrioxamine B with selected heavy metal cations. *Inorganica Chimica Acta*, **244**, 179–184.

Hersman, L., Lloyd, T. and Sposito, G. (1995) Siderophore-promoted dissolution of hematite. *Geochimica et Cosmochimica Acta*, **59**, 3327–3330.

Holmén, B.A. and Casey, W.H. (1996) Hydroxamate ligands, surface chemistry, and the mechanism of ligand promoted dissolution of goethite [α-FeOOH(s)]. *Geochimica et Cosmochimica Acta*, **60**, 4403–4416.

Holmén, B.A., Tejedor-Tejedor, M.I. and Casey, W.H. (1997) Hydroxamate complexes in solution at the goethite-water interface: a cylindrical internal reflection Fourier transform infrared spectroscopy study. *Langmuir*, **13**, 2197–2206.

Kalinowski, B.E., Liermann, L.J., Brantley, S.L., Barnes, A. and Pantano, C.G. (2000) X-ray photoelectron evidence for bacteria-enhanced dissolution of hornblende. *Geochimica et Cosmochimica Acta*, **64**, 1331–1343.

Konetschny-Rapp, S., Jung, G., Raymond, K.N., Meiews, J. and Zahner, H. (1992) Solution thermodynamics of the ferric complexes of new desferrioxamine siderophores obtained by directed fermentation. *Journal of the American Chemical Society*, **114**, 2224–2230.

Kraemer, S.M. (2004) Iron oxide dissolution and solubility in the presence of siderophores. *Aquatic Sciences*, **66**, 3–18.

Kraemer, S.M., Cheah, S.-F., Zapf, R., Xu, J., Raymond, K.N. and Sposito, G. (1999) Effect of hydroxamate siderophores on Fe release and Pb(II) adsorption by goethite. *Geochimica et Cosmochimica Acta*, **63**, 3003–3008.

Kraemer, S.M., Xu, J., Raymond, K.N. and Sposito, G. (2002) Adsorption of Pb(II) and Eu(III) by oxide minerals in the presence of natural and synthetic hydroxamate siderophores. *Environmental Science and Technology*, **36**, 1287–1291.

Liermann, L.J., Kalinowski, B.E., Brantley, S.L. and Ferry, J.G. (2000) Role of bacterial siderophores in dissolution of hornblende. *Geochimica et Cosmochimica Acta*, **64**, 587–602.

Martell, A.E. and Smith, R.E. (2001) *NIST Stability Constants of Metal Complexes Database* 46, version 6.0, US Department of Commerce, Gaithersburg, Maryland.

Meiwes, J., Fiedler, H.P., Zahner, H., Koneschny-Rapp, S. and Jung, G. (1990) Production of desferrioxamine-E and new analogs by direct fermentation and feeding fermentation. *Applied Microbiology and Biotechnology*, **32**, 505–510.

Neilands, J.B. (1981) Microbial iron compounds. *Annual Reviews Biochemistry*, **50**, 715–732.

Neubauer, U., Nowack, B., Furrer, G. and Schulin, R. (2000) Heavy metal sorption on clay minerals affected by the siderophore desferrioxamine B. *Environmental Science and Technology*, **34**, 2749–2755.

Parkhurst, D.L. and Appelo, C.A.J. (1999) *User's guide to PHREEQC (version 2) – a computer program for speciation, batch-reaction, one-dimensional transport, and inverse geochemical calculations*. USGS Water-Resources Investigations Report 99-4259.

Rosenberg, D.R. and Maurice, P.A. (2003) Siderophore adsorption to and dissolution of kaolinite at pH 3 to 7 at 22ºC. *Geochimica et Cosmochimica Acta*, **67**, 223–229.

Ruggiero, C.E., Matonic, J.H., Reilly, S.D. and Neu, M.P. (2002) Dissolution of plutonium(IV) hydroxide by desferrioxamine siderophores and simple organic chelators. *Inorganic Chemistry*, **41**, 3593–3595.

Sutheimer, S.H., Maurice, P.A. and Zhou, Q. (1999) Dissolution of well and poorly crystallized kaolinites: Al speciation and effects of surface characteristics. *American Mineralogist*, **84**, 620–628.

(*Received 4 August 2004; revised 2 February 2005; Ms. 947; A.E. Javiera Cervini-Silva*)